NUMERICAL ANALYSIS OF MIXED CONVECTION FLOW AND HEAT TRANSFER IN A LID-DRIVEN OCTAGONAL CAVITY WITH HEATING ON TWO SIDEWALLS

Mushtaq F. Al-Mensorey

Department of Mechanical Engineering, College of Engineering, University of Al-Qadissiya, Iraq.

Email: mushtaq.almensory@gmail.com

Received 9 September 2015 Accepted 21 September 2015

ABSTRACT

This paper numerically investigates laminar mixed convection flow through an octagonal cavity enclosure where four cases with different positions and directions of its lid-driven were simulated. The lid-driven moves in horizontal rightward and leftward on its upper wall in the first and second cases while it moves vertical upward and downward on its right side wall in the others cases. The numerical study was carried out by solving the governing equations (continuity, momentum and energy), and applying the tri-diagonal matrix algorithm (TDMA) method via ANSYS 11.0 program. Four of the eight external walls of the octagonal cavity enclosure are insulation walls and the other four walls were classified into two hot and two cold walls. The mixed convection flow and heat transfer characteristics through isotherms, streamlines and the average Nusselt number were considered based on different Richardson numbers (Ri = 0.01, 1, and 10). The results demonstrated that heat transfer mechanism, the flow pattern and formation of vortices are significantly dependent on values of the Richardson number. Within the enclosure, the lid-driven movements showed an improvement in the heat transfer rate where the direction of the sliding wall considerably affected the flow and temperature distributions for all values of the Richardson number. The Nusselt number of the lid-driven increased from 50 with the upward motion to 55 (10 % increase rate) with the downward motion counterpart, and increased from 12 to 17 (40 % increase rate) with the rightward and the leftward motions, respectively.

Keywords: mixed convection, octagonal cavity, lid-driven, tri-diagonal matrix algorithm (TDMA).

التحليل العددي للحمل الحراري والجريان المختلط في تجويف ثماني ذو غطاء متحرك وحرارة من جانبين

م.م. مشتاق فيصل المنصوري

الخلاصة:

في هذا البحث, تم انجاز التحليل العددي للحمل الحراري والجريان المختلط خلال تجويف ثماني الشكل , حيث تمت محاكاة أربع حالات ذات مواقع واتجاهات مختلفة للغطاء المتحرك. الحالات الاربعة تتمثل بحركتين افقيتين نحو اليمين ونحو اليسار للجدار العلوي للغطاء وحركتين عموديتين صعودا وهبوطا للجدار الأيمن للغطاء المتحرك. أجريت الدراسة العددية من خلال حل المعادلات الحاكمة (الاستمرارية، الزخم، والطاقة) وتطبيق طريقة الخوارزمية ذات الثلاث اقطار (TDMA) باستخدام برنامج ANSYS 11.0. أربعة من الثمان جدران الخارجية للتجويف المثمن هم جدران معزولة والجدران الأربعة الأخرى هم جداران ساخنان واخران باردان. واعتمد تأثير التدفق الحراري المختلط وخصائص انتقال الحرارة على مخططات الحرارة و خطوط

الجريان ومعدل عدد نسلت بناءأ على أرقام مختلفة لريتشاردسون (Ri=0.01, 1, and 10). أظهرت النتائج أن آلية انتقال الحرارة ونمط التدفق فضلا عن تشكيل الدوامات تعتمد بشكل كبير على قيم عدد ريتشاردسون وان حركة الغطاء تُحسن معدل انتقال الحرارة وان اتجاه الجدار المنزلق (المتحرك) يؤثر بشكل كبير على تدفق وتوزيع درجات الحرارة داخل التجويف لجميع اعداد ريتشاردسون، أن عدد نسلت ازداد من 50 (معدل زيادة 10 %) مع الحركة العمودية باتجاه الاعلى الى 55 مع الحركة العمودية باتجاه الأسفل ومن 12 (معدل زيادة 40 %) مع الحركة الافقية باتجاه اليمين الى 17 باتجاه اليسار.

NOMENCLATURE:

Symbol	Description	Unit	Symbol	Description (Greek Symbols)	Unit
C_p	*Specific Heat*	*J/kg.°C*	α	*Thermal Diffusivity*	m^2/s
g	*Gravitational Acceleration*	m/s^2	β	*Volumetric Coefficient of Thermal Expansion*	K^{-1}
h_f	*Film Coefficient*		μ	*Viscosity*	$N.s/m^2$
k	*Thermal Conductivity of Fluid*	*W/m. °C*	ν	*Kinematic Viscosity of the Fluid*	m^2/s
L	*Side Length*	*m*	ρ	*Density of the Fluid*	kg/m^3
Nu	*Average Nusselt Number*		Ψ	*Stream Function*	m^2/s
p	*Pressure*	N/m^2	$\{\eta\}$	*Unit Out Ward Normal Vector*	
Pr	*Prandtl Number,* $Pr=\nu/\alpha$		α	*Thermal Diffusivity*	m^2/s
q	*Heat Flux*	*watt*	β	*Volumetric Coefficient of Thermal Expansion*	K^{-1}
$\{q\}$	*Heat Flux Vector*		μ	*Viscosity*	$N.s/m^2$
Ri	*Richardson Number*		ν	*Kinematic Viscosity of the Fluid*	m^2/s
T	*Temperature*	*°C*			
	Bulk Temperature of the adjacent fluid	*°C*			
T_s	*Temperature of the surface of the model*	*°C*			
V_x	*Velocity Component in x-Direction*	*m/s*			
V_y	*Velocity Component in y-Direction*	*m/s*			
X	*Cartesian Coordinate in Horizontal Direction*	*m*			
Y	*Cartesian Coordinate in Vertical Direction*	*m*			

INTRODUCTION

The flow and heat transfer of a lid-driven enclosure have taken a considerable interest in the recent years due to their uses in the industrial and thermal instruments such as solar collector, heat exchangers, and cooling of electronic devices [1]. Also, the combined mixed convection flow and heat transfer find its applications in float glass production, material processing, crystal growth, metal coating and casting [2]. In order to extensively understand the thermal performance and heat transfer of the mixed convection flow in a lid-driven enclosure, numerous modeling and simulation

studies considering both the buoyancy force and the shear force caused by the wall motion of the cavity have been published in the literature. For example, Sivasankaran et al. [3] numerically investigated the mixed convection flow in a square cavity with temperature on both vertical sides. They found that the non-uniform heating on one wall gave lower heat transfer rate than that for heating on both walls. Cheng and Liu [2] also investigated the effect of horizontal and vertical temperature gradients on the flow and heat transfer behavior of mixed convection in a square cavity for different Richardson numbers. The laminar mixed convection flow in a square cavity with variations of the average Nusselt number was numerically simulated using ANSYS FLUENT commercial CFD code by Akand et al. [4]. It was noticed that the Nusselt number does not clearly vary with increasing Richardson number till it approaches the value of 1 with which the average Nusselt number rapidly increased.

Furthermore, several numerical studies such as Ghasemi and Aminossadati [5] and Ching et al. [6] indicated the heat transfer and fluid flow of mixed convection in a lid-driven triangle enclosure. They found that the thermal performance of a triangle enclosure filled with water strongly affected with the pertinent parameters i.e., direction of the vertical sliding wall, Richardson number and solid volume fraction. The effects of inclination angle and Richardson number as well as aspect ratio on the heat transfer in a air-filled square cavity were numerically simulated by Cheng and Liu [7], and on heat transfer in a rectangular inclined channel by Marroquin et al. [8]. The heat transfer in an inclined lid-driven enclosure with different magnetic field angles was investigated by Mondal and Sibanda [9]. The simulation results showed that the increase of inclination angle does not affect the flow and heat transfer when the flow is in a forced convection dominated regime (Ri = 0.01). Nevertheless, the laminar mixed convection flow and heat transfer inside an octagonal lid-driven enclosure has not been studied yet. Thus, this investigation attempts to address the effects of several pertinent parameters such as the horizontal and vertical sliding wall motions, Richardson number and the position of lid-driven whether right or top side on the thermal performance and heat transfer of the octagonal cavity. The numerical analysis was done based on solving the governing equations (Continuity, Momentum and Energy Equations) and using the tri-diagonal matrix algorithm (TDMA) method via ANSYS 11.0 program.

MODEL DESCRIPTION AND EQUATIONS

An octagonal cavity shape with four insulated walls, two hot and two cold walls as schematically shown in **Figure 1** was used in this study. The right and left walls of the octagonal cavity are adopted as hot walls with T_h, and the top and bottom walls are adopted as cold walls with T_c. Based on the position and the direction of the lid-driven, four different cases were considered in the analysis (see **Figure 1**). The case 1 adopts the horizontal top lid-driven, moving towards the right hand side; the case 2 is the same as the case 1 expect that its lid-driven is moving towards the left hand side. The case 3 considers the vertical right hand side of the lid-driven, moving upwards, and the case 4 is similar to case 3 expect that its lid-driven is moving downwards. The working fluid used in the cavity is air with Pr=0.71 and constant properties. The two-dimensional governing equations (continuity, the momentum and energy equations) [3] based on a steady state one phase and laminar incompressible buoyancy-induced flow were solved by using the commercial ANSYS 11.0 program as follows:

Continuity equation [3]:

$$\frac{\partial(\rho V_x)}{\partial x}+\frac{\partial(\rho V_y)}{\partial y}=0 \tag{1}$$

Momentum equations [3]:

$$\frac{\partial(\rho V_x V_x)}{\partial \mathrm{x}}+\frac{\partial(\rho V_y V_x)}{\partial \mathrm{y}}=\rho g_x-\frac{\partial \mathrm{P}}{\partial \mathrm{x}}+\frac{\partial}{\partial \mathrm{x}}\left(\mu\frac{\partial V_x}{\partial x}\right)+\frac{\partial}{\partial y}\left(\mu\frac{\partial V_x}{\partial y}\right) \tag{2}$$

$$\frac{\partial(\rho V_x V_y)}{\partial x}+\frac{\partial(\rho V_y V_y)}{\partial y}=\rho g_y-\frac{\partial \mathrm{P}}{\partial \mathrm{y}}+\frac{\partial}{\partial \mathrm{x}}\left(\mu\frac{\partial V_y}{\partial x}\right)+\frac{\partial}{\partial y}\left(\mu\frac{\partial V_y}{\partial y}\right) \tag{3}$$

Energy equation [3]:

$$\frac{\partial}{\partial \mathrm{x}}\left(\rho V_x C_p T\right)+\frac{\partial}{\partial y}\left(\rho V_y C_p T\right)=\frac{\partial}{\partial x}\left(k\frac{\partial T}{\partial x}\right)+\frac{\partial}{\partial y}\left(k\frac{\partial T}{\partial y}\right) \tag{4}$$

where V_x and V_y are the velocity components in the x and y direction, respectively; P is the pressure and T is the temperature.

The boundary conditions applied to the computational model are assumed as follows:

(i) Velocity

$V_x = V_y = 0$ at all constant walls except that of the moved wall (lid-driven).

The variables U and –U refer to velocities of the horizontal lid-driven rightward and leftward directions, respectively.

The variables V and –V refer to velocities of the vertical lid-driven upward and downward directions, respectively.

(ii) Temperature

$T=T_h$ is assumed for all vertical right and left walls, and

$T=T_c$ is assumed for all horizontal top and bottom walls.

(iii) Stream function

Stream function for two-dimensional structure is computed based on the following equation [3]:

$$\frac{\partial \psi}{\partial \mathrm{X}}=-\rho V_Y \quad \text{and} \quad \frac{\partial \psi}{\partial \mathrm{Y}}=\rho V_X \tag{5}$$

Local Nusselt number is chosen as an indicator for the heat transfer rate for the purpose of determining the effect of several parameters on the heat transfer. The local Nusselt number is defined as:

$$Nu_l = \frac{h_f L}{k} \quad (6)$$

, and the (h_f) is obtained from the following equation

$$\{q\}^T \{\eta\} = h_f (T_s - T_B) \quad (7)$$

Richardson number (Ri) is dimensionless which can be obtained from:

$$Ri = \frac{Gr}{\mathrm{Re}^2} \quad (8)$$

where

$$Gr = \frac{g\beta(T_h - T_c)L^3}{\nu}, and \qquad \mathrm{Re} = \frac{uL}{\nu}$$

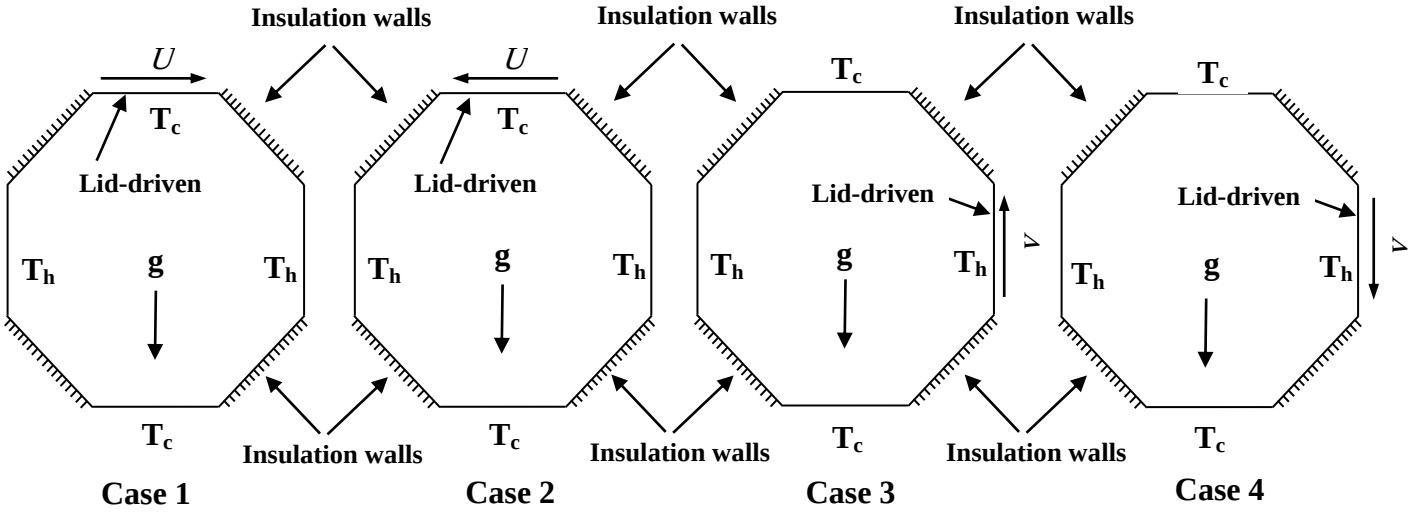

Figure (1): Physical model and boundary conditions for four

3. Numerical solution

Over the computational domain, the grid system was done by unstructured quadratic elements, four nodes which are unevenly distributed close to edge of the octagonal cavity enclosure where higher grid densities are desired as shown in **Fig. 2**. The four nodes quadric elements of 43200 were chosen for their more accurate results and low error tolerance. The governing equations are solved with the convergence iteration of 10^{-8} for each variable, and integrated over the domain with use of the exponential interpolation in the mean flow direction inside the finite element. Using the finite element ANSYS 11.0 program and employing the tri-diagonal matrix algorithm (TDMA), the governing differential equations (continuity, momentum and energy equations) were solved. The theory of TDMA algorithm is based on dividing the problem into a series of tri-diagonal problems. For a completely unstructured mesh, or an arbitrary numbered system, the TDMA method reduces

to the Gauss-Seidle iterative method and set of algebraic equations is solved based on the successive under relaxation (SUR) technique where the 0.1 is taken as an under relaxation parameter. Further details about the TDMA method can be found in Patanker [10]. The grid independence test is normally applied to ensure the accuracy of the numerical results and determine the approach grid density. In comparison of the average Nusselt number with number of nodes, the average Nusselt number determined by the **Eq. 6** is constant when number of nodes reached the 50,000 and higher as shown in **Fig. 3**.

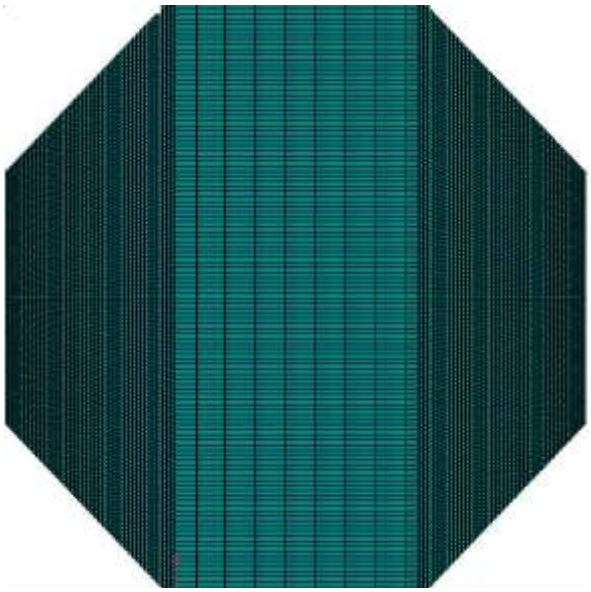

Figure (2): A distinctive grid distribution with quadratic elements.

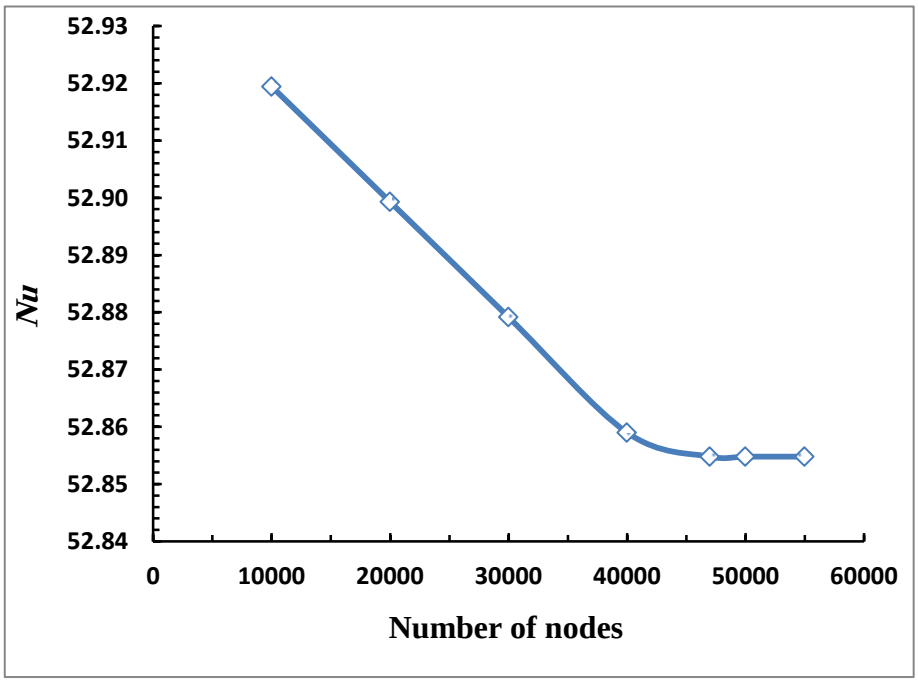

Figure (3): Relationship between the average Nusselt number and number of nodes.

RESULTS AND DISCUSSION

Results of the effects of horizontal and vertical sliding wall motion and the position of lid-driven with three Richardson numbers (Ri =0.01, 1, and 10) based on magnitudes of the velocity of lid-driven on the streamline, temperature and velocity distribution as well as Nusselt number inside the octagonal enclosure are presented in the following sections.

1 Top horizontal rightward motion of the lid-driven (Case 1).

1.1 Flow field (streamline)

Figure 4a shows the behavior of vortex of the flow field (flow pattern) for Ri = 0.01 that gives high velocity when applying the **Eq. 8**. It can be noticed that a single vortex generated inside the cavity due to the high velocity of lid-driven that resulted in frictional losses and stagnation pressure [2]. The direction of horizontal rightward motion of the lid-driven which moves tangentially with the vortex causing in a clockwise recirculation of the vortex. It can be also observed that the minimum value of the vortex is at the middle of the cavity, and the maximum value of the vortex is near the walls. The region of the fluid streamfunctions near the top moved lid-driven wall is almost smaller than this near the others walls. This behavior is attributed again to the effect of the high velocity of the lid-driven [11]. As Ri is increased to 1.0 (**Fig. 4b**), the effect of lid-driven on the flow pattern becomes less stronger and the velocity is slower than that of Ri=0.01. However, the mechanically-driven top lid resulted in the generation of two - top and bottom - vortices inside the cavity plays an important role in increasing the heat transfer rates. These two vortices are approximately in equal size and generated due to presence of free convection and its role that has become nearly equilibrium with the role of force convection. Muthtamilselvan and Doh [12] found that Richardson number strongly affect the fluid flow and heat transfer in the cavity and the forced convection becomes dominant in the entire cavity. The top vortex moves in clockwise direction due to the effect of lid-driven motion and the effect of hot wall on the left side whereas the bottom vortex moves in counterclockwise due to the role of free convection resulted from the hot wall on the right side. When Ri is further increased to 10 (**Fig. 4c**), the effect of the lid-driven motion is also caused in generating two top and bottom vortices but they are in different sizes and rotate in different directions.

1.2 Isothermal field (temperature distribution)

The effect of top horizontal rightward motion of the mechanically-driven lid (Case 1) on the isotherm patterns (temperature distribution) for Ri = 0.01, 1, and 10 is shown in **Fig. 4 d-f**. In term of Ri = 0.01 (**Fig. 4d**), the thermal boundary layer was observed on the hot right and left walls with a small thickness at the top part of the hot right wall. This thickness increased gradually to reach the maximum at the bottom of the same wall. At the hot left wall, the thickness of thermal boundary layer is small at the bottom part of the wall and it increased gradually at the top side of the wall. This is mainly due to the effect of moving air velocity that resulted from the high velocity of the lid-driven which, in turn controls the heat transfer from the hot walls to inside the cavity. With increasing Ri to 1 (**Fig. 4e**), the thickness of the thermal boundary layer on the hot wall and the free convection is also increased, leading to maintain a nearly equilibrium between free convection and force convection due to the reduction of the lid-driven velocity. Further increasing of Ri into 10, the temperature distribution becomes more obvious than that with the Ri = 1 as shown in **Fig. 4f**. This is ascribed to decrease the influence of the lid-driven velocity which means that the free convection is the dominant heat transfer method inside the cavity [13].

1.3 Velocity field

Figure 4g shows the velocity distribution of the fluid flow inside the cavity for $\mathrm{Ri} = Gr/\mathrm{Re}^2 = 0.01$. For this designated Ri number, the velocity is the highest and the velocity boundary layer is small near the moved lid-driven wall due to the high velocity of the fluid that restricted the expansion of the layer.

On the opposite, it can be seen from the **Fig. 4g** that the velocity value is zero near the others walls and at the middle of the cavity. Increasing the Ri number to 1.0 (**Fig. 4h**), the impact of the lid-driven motion on the velocity is less stronger and hence the region of the velocity boundary layer and the velocity distribution are larger than which for the Ri=0.01 due to the role of free convection that becomes more effective in this case. The velocity distribution of the fluid is further increased and the lid-driven velocity is further decreased with increasing Ri to 10 as shown in **Fig. 4i**. This is contributed in the dominance of free convection in the cavity and increasing the heat transfer rates, this finding is in conformance with that was noted in Khanafer's study [14]. The maximum velocity was noted to be reached at the contact region between the two vortices while the minimum velocity is occurred at the center of two vortices and near all walls except the sliding wall.

2 Top horizontal leftward motion of the lid-driven (Case 2).

2.1 Flow field (streamline)

In this case, the effect of the top horizontal leftwards motion of the lid-driven for three Richardson numbers (0.01, 1, and 10) on the flow patterns and behavior of vortices of the flow field is illustrated in **Fig. 5a-c**. In terms of Ri = 0.01 (**Fig. 5a**), as previously discussed within Case 1, a primary vortex is generated inside the cavity due to the high velocity of the lid-driven that moves leftwards, recirculating the vortex counterclockwise. The value of the vortex is maximized in the middle of the cavity and it is minimized near the walls. The region of the fluid streamfunctions near the sliding lid-driven wall is approximately smaller than this near the others walls. This is due to the effect of the high velocity of the lid-driven. When Ri is increased to 1.0 (**Fig. 5b**), the effect of lid-driven on the flow field becomes less effective and the velocity becomes lower than that with Ri=0.01. However, this mechanically-driven top lid motion resulted in building two vortices inside the cavity enclosure due to the role of free convection which becomes nearly equilibrium with the role of force convection. These two upper-right and lower-left vortices are almost having similar sizes. The upper-right vortex moves counterclockwise owing to the effect of lid-driven motion and the effect of hot wall on the right side while the lower-left vortex moves clockwise due to the role of free convection that resulted from the hot wall on the left side. As Ri is further increased to 10 (**Fig. 5c**), the effect of the lid-driven motion is also resulted in building two upper-right and lower-left vortices but they are in different sizes and rotate in different directions.

2.2 Isothermal field (temperature distribution)

The effect of top horizontal leftwards motion of mechanically-driven lid (Case 2) on the isotherm field (temperature distribution) for Ri = 0.01, 1, and 10 is shown in **Fig. 5 d-f**. For the Ri = 0.01 (**Fig. 5d**), the thermal boundary layer was seen on the hot right and left walls with a minimum thickness at the lower part of the hot right wall and gradually increased to reach the maximum at the upper part of the same wall. At the hot left wall, the thickness of thermal boundary layer is small at the upper part of the wall and it gradually increases at the lower part of the same wall. This is mainly due to the effect of velocity of the moved air that induces dominant of force convection in the entire cavity. With increasing Ri to 1 (**Fig. 5e**), the thickness of the thermal boundary layer on the hot wall is also increased due to the reduction of the lid-driven velocity which leads to increase

the free convection and maintain the nearly equilibrium between free convection and force convection. Further increase of Ri to 10, the temperature distribution becomes more obvious than that with the Ri = 1 as shown in **Fig. 5f**. This is ascribed to vanish the role of the lid-driven velocity which means that the free convection is dominant inside the entire cavity.

2.3 Velocity field

Figure 5g shows the velocity distribution of the fluid flow inside the cavity for Ri = 0.01 where the velocity is the highest and the velocity boundary layer is small near the moved lid-driven wall. In contrast, it can be seen from the **Fig. 5g** that the velocity value is zero near the others walls and at the middle of the cavity. Increasing Ri to 1.0 (**Fig. 5h**), the role of the lid-driven motion on the velocity is less effective and hence the region of the velocity boundary layer and the velocity distribution are larger than which for Ri=0.01 owing to the role of free convection that becomes more effective in this case. The velocity distribution of the fluid is further increased and the lid-driven velocity is further decreased with increasing Ri to 10 as shown in **Fig. 5i**. This is contributed in the dominance of free convection in the cavity and increasing the heat transfer rates. The maximum velocity was noted to be reached at the contact region between the two vortices while the minimum velocity is occurred at the center of two vortices and near all walls except the sliding wall.

3 Right vertical upward motion of the lid-driven (Case 3).

3.1 Flow field

Figure 6a shows the flow pattern (streamline) for Ri=0.01 and the right vertical upward motion of the lid-driven that moves in a high velocity. It can be seen that a large single vortex is generated inside the entire cavity which is rotated anticlockwise direction. The minimum value of the vortex (fluid streamfunctions) seems to be near the walls and its region which is near the hot right moved lid-driven wall, is almost smaller than this near the others walls while the maximum region is at the middle of the cavity enclosure. When Ri=1 (**Fig. 6b**), the single vortex seems to be a semi-elliptical shape approaching the right sliding wall due to the increased effective of the free convection. Meanwhile, the region of the minimum streamfunction in the hot left wall of the cavity increased. As the Ri increased to 10 (**Fig. 6c**), the effect of free convection in the entire cavity becomes dominant, leading to increase the deformation of the vortex which discussed in the previous case (**Fig. 6b**) that resulted in separating the single vortex into two vortices [7]. The generated vortices are in different sizes and rotating in two different directions. The larger vortex locates close to the hot sliding wall and rotates anticlockwise whereas the other vortex locates on the hot left wall and rotates clockwise. Similarly, this was also revealed in the Esfe et al.'s work [15] where they were seen the vortex migration to higher positions inside the cavity occurred and higher heat transfer rates obtained due to the change in the Ri number and then the lid-driven velocity.

3.2 Isothermal field

The isothermal field (temperature distribution) for Ri=0.01 is shown in **Fig. 6d**. It can observe that the thermal boundary layer is contiguous on the hot right sliding wall and it is widely expanded to reach its maximum thickness at the adjacent insulated top wall. This is attributed to the direct effect of the mechanically-driven lid on the hot right wall. However, this layer is in its minimum thickness at the hot top left wall and it is gradually expanded approaching the bottom of the same wall. When Ri=1 (**Fig. 6e**), the temperature distribution is more obvious than that for Ri = 0.01 due the reduced velocity of the lid-driven that caused in the occurrence of semi-equilibrium case

between the free and force convection flow. With further increase of Ri to 10 (**Fig. 6f**), the temperature distribution became semi symmetric around the vertical axis owing to the decreased effect of a lid-driven velocity. In other words, the free convection dominates the entire cavity.

3.3 Velocity field

Figure 6g shows the velocity distribution of the fluid flow inside the cavity for Ri = 0.01 where the velocity is the highest and the thickness of velocity boundary layer is small near the right upwards sliding wall whereas the velocity value is zero near the others walls and at the middle of the cavity. When Ri = 1 (**Fig. 6h**), the effect of lid-driven velocity is lesser and the velocity distribution inside the entire cavity is wider than those for Ri=0.01 owing to the role of free convection that becomes more effective. Consequently, the thickness of velocity boundary layer is expanded on the sliding wall and the stagnation region is increased at the hot bottom left wall. Moreover, the lid-driven velocity is further decreased and the velocity distribution of the fluid is further increased with increasing Ri to 10 as illustrated in **Fig. 6i**. This is ascribed to the free convection that dominated the entire cavity. The maximum velocity emerged to be in the middle of the octagonal enclosure and the minimum velocity is at the centers of the generated vortices and near all the walls except the hot right lid-driven. The velocity distribution is a semi-symmetric around the vertical axis with a small deformation due to the force convection.

4 Right vertical downward motion of the lid-driven (Case 4).

4.1 Flow field

Figure 7a shows the flow field for Ri=0.01 under right vertical downward motion of a lid-driven. It is demonstrated that a large single vortex is generated inside the cavity rotates clockwise due to the high velocity of the sliding wall. The minimum value of the vortex (fluid streamfunctions) seems to be in the middle of the cavity while the maximum value is near the walls. The minimum region of the flow pattern is near the hot right downwards sliding wall and the maximum region is near the others walls due to the dominance of the force convection [16]. With increasing Ri to 1, the large single vortex is split into three longitudinal vortices (see **Fig. 7b**) with different sizes due to the increased effect of free convection that resulted in a semi-equilibrium between free and force convection heat transfer mechanism. The largest vortex locates near the hot left sliding wall and moves in clockwise direction for the difference in hot and cold temperatures on the walls. The second vortex generated due to the effect of the free and force convection, locates in the middle of the cavity and rotates anticlockwise. The third vortex that lies near the hot right wall and rotates clockwise, generated owing to the force convection. The latter vortex is almost vanished and the two former vortices are enlarged with increasing Ri to 10 as shown in **Fig. 7c**. In this case, the free convection is dominated in the cavity.

4.2 Isothermal field

Figure 7d shows the thermal boundary layer for Ri=0.01 is contiguous on the hot right sliding wall and widely expanded to reach its maximum thickness at the adjacent insulated bottom wall due to the direct effect of the mechanically-driven lid on the hot right wall. However, the minimum thickness of the layer is shown on the hot bottom left wall and it is gradually expanded approaching the top of the same wall. As Ri increased to 1 (**Fig. 7e**), the temperature distribution is more obvious than that for Ri = 0.01 due the decreased velocity of the lid-driven that resulted in the occurrence of semi-equilibrium case between the free and force convection. With further increase of Ri to 10 (**Fig. 7f**), the temperature distribution became semi symmetric around the vertical axis

due to the reduced effect of a lid-driven velocity which means that the free convection dominated the cavity.

4.3 Velocity field

The velocity distribution of the fluid flow inside the cavity for Ri = 0.01 is shown in **Fig. 7g**. The velocity is the highest and the thickness of velocity boundary layer is small near the right downward lid-driven while the velocity value is zero near the others walls and at the middle of the octagonal cavity. When Ri=1 (**Fig. 7h**), the effect of lid-driven velocity is lesser and the velocity distribution inside the cavity is wider than that for Ri=0.01 due to the role of free convection that becomes more effective. As a result, the thickness of velocity boundary layer is expanded on the sliding wall and the stagnation region is increased at the hot bottom right wall. Additionally, the velocity is further reduced and the velocity distribution of the fluid is further increased when Ri = 10 as shown in **Fig. 7i**. This behavior is occurred for the free convection that dominated the entire cavity. The maximum velocity emerged to be in the middle of the octagonal cavity and the minimum velocity is at the centers of the vortices and near all the walls except the sliding wall. The velocity distribution is a semi-symmetric around the vertical axis with a small deformation due to the force convection.

Heat transfer field

The variation in the Nusselt number (Nu) of the mixed convection flow for Ri= 0.01, 1, 10 and different locations along the hot right wall was calculated and compared in **Fig. 8**. For which, four different directions i.e., rightward, leftward, upward, and downward of the lid-driven were considered. The designated hot right wall was equally partitioned into numerous grids in order to calculate the average Nu in different positions. The calculated Nu exhibited that the heat transfer rate at the hot right wall increases with decreasing Ri. The lid-driven moving towards left (case 2) had a better heat transfer rate than the lid-driven moving rightwards (case 1). This is due to the increased buoyancy effect and the increased air velocity inside the cavity [2]. Similarly, the lid-driven moving downwards (case 4) had a better heat transfer rate than the lid-driven was moving to upward (case 3). The vertical motion of the lid-driven whether upwards or downwards significantly increases the heat transfer rates compared to the horizontal motion (rightwards or leftwards) that exhibited a less effective on the heat transfer rates. In light of the relation of fluid motion and shape of the octagonal cavity on the heat transfer rate; it was shown that such a shape tends to generate a single circular vortex with the use of smaller Ri. With higher Ri values, the single vortex separated into two or three vortices due to the reduction of velocity. This is resulted in significant increases of the heat transfer rates.

Conclusion

The mixed convection flow and heat transfer in a lid-driven octagonal cavity filled with air fluid was numerically studied using ANSYS 11.0 program. The horizontal rightwards, leftwards and vertical, upwards and downwards directions were considered. The effect of different positions and directions of the sliding wall and Richardson number on the flow, temperature fields and heat transfer rate was examined. The results revealed the following findings:

- The flow pattern, temperature and velocity have significantly changed with changing Ri numbers and the motion of the lid-driven.
- Any motion in the lid-driven showed an improvement in the heat transfer rate of the cavity.

- For all Richardson numbers, the vertical downward and the horizontal leftward lid-driven motions proved to have higher heat transfer rates compared to the vertical upward and the horizontal rightwards lid-driven motions, respectively.
- The higher heat transfer rates increased with decreasing the Richardson number for the strengthening of flow circulation due to effects of the sliding wall motion.

References

[1] Chin-Hsiang Cheng, Chin-Lung Chen, " Buoyancy-induced periodic flow and heat transfer in lid-driven cavities with different cross-sectional shapes", *International Communications in Heat and Mass Transfer* 32 (2005) 483-490.

[2] T.S. Cheng, W.-H. Liu, " Effect of temperature gradient orientation on the characteristics of mixed convection flow in a lid-driven square cavity", *Computers & Fluids* 39 (2010) 965-978.

[3] S. Sivasankaran, V. Sivakumar and P. Prakash," Numerical study on mixed convection in a lid-driven cavity with non-uniform heating on both sidewalls", International Journal of Heat and Mass Transfer 53 (2010) 4304-4315.

[4] Akand W. Islam, Muhammad A.R. Sharif, Eric S. Carlson, "Mixed convection in a lid driven square cavity with an isothermally heated square blockage inside", International Journal of Heat and Mass Transfer 55 (2012) 5244–5255.

[5] B. Ghasemi, S. M. Aminossadati, " Mixed convection in a lid-driven triangle enclosure filled with nanofluids", International Communications in Heat and Mass Transfer 37 (2010) 1142-1148.

[6] Y.C. Ching, Hakan F. Öztop, M.M. Rahman, M.R. Islam, A. Ahsan, " Finite element simulation of mixed convection heat and mass transfer in a right triangular enclosure", International Communications in Heat and Mass Transfer 39 (2012) 689–696.

[7] T.S. Cheng, W.-H. Liu, " Effects of cavity inclination on mixed convection heat transfer in lid-driven cavity flows", Computers & Fluids 100 (2014) 108–122.

[8] J. Marroquin-Desentis, C. Trevino, J.C. Cajas, E. Salcedo, L. Martinez-Suastegui," Numerical study on buoyancy and inclination effects on transient laminar opposing mixed convection in rectangular channels with symmetric and discrete heating", International Journal of Heat and Mass Transfer 84 (2015) 766–785.

[9] Sabyasachi Mondal, Precious Sibanda," Unsteady double diffusive convection in an inclined rectangular lid-driven enclosure with different magnetic field angles and non-uniform boundary conditions", International Journal of Heat and Mass Transfer 90 (2015) 900–910.

[10] S.V. Patankar," Numerical Heat Transfer and Fluid Flow", Hemisphere publishing corporation, New York, 1980.

[11] M. Hasanuzzaman, M.M. Rahman, Hakan F. Öztop, N.A. Rahim, R. Saidur, "Effects of Lewis number on heat and mass transfer in a triangular cavity", International Communications in Heat and Mass Transfer, 39 (2012) 1213–1219.

[12] M. Muthtamilselvan, Deog Hee Doh, "Mixed convection of heat generating nanofluid in a lid-driven cavity with uniform and non-uniform heating of bottom wall", Applied Mathematical Modelling, 38 (2014) 3164–3174.

[13] S. Gumgum, M. Tezer-Sezgin, "DRBEM solution of mixed convection flow of nanofluids in enclosures with moving walls", Journal of Computational and Applied Mathematics, 259, Part B (2014) 730–740.

[14] Khalil Khanafer, "Comparison of flow and heat transfer characteristics in a lid-driven cavity between flexible and modified geometry of a heated bottom wall", *International Journal of Heat and Mass Transfer*, 78 (2014) 1032–1041.

[15] Mohammad Hemmat Esfe, Mohammad Akbari, Arash Karimipour, Masoud Afrand, Omid Mahian, and Somchai Wongwises, "Mixed-convection flow and heat transfer in an inclined cavity equipped to a hot obstacle using nanofluids considering temperature-dependent properties", *International Journal of Heat and Mass Transfer*, 85 (2015) 656–666.

[16] M. Borhan Uddin, M.M. Rahman, M.A.H. Khan, Talaat A. Ibrahim, " Effect of buoyancy ratio on unsteady thermosolutal combined convection in a lid driven trapezoidal enclosure in the presence of magnetic field", *Computers & Fluids*, 114 (2015) 284–296.

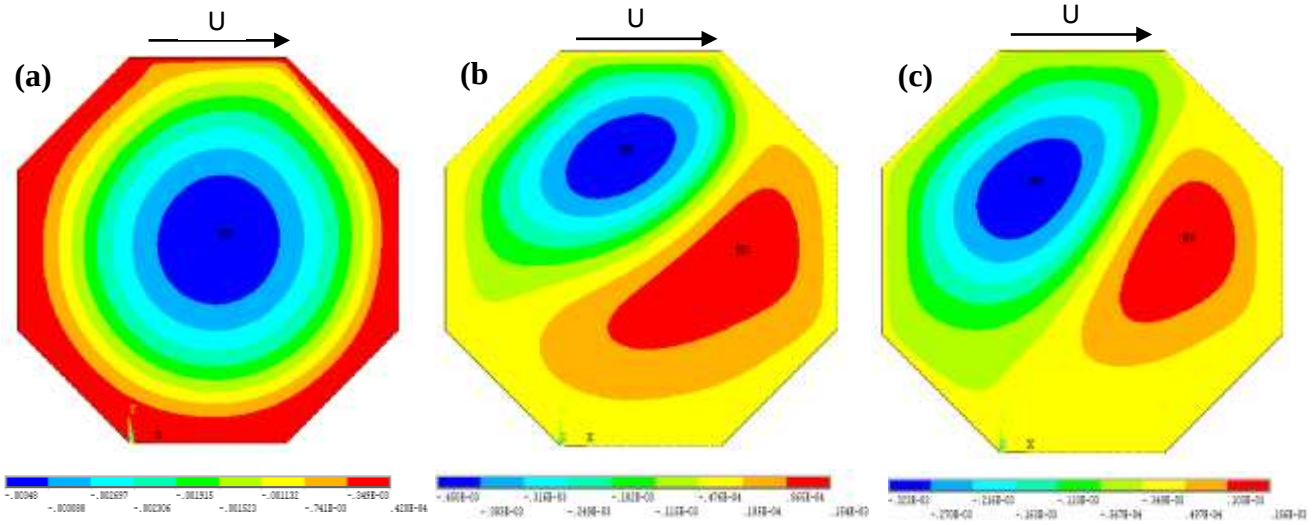

Stream function body contour

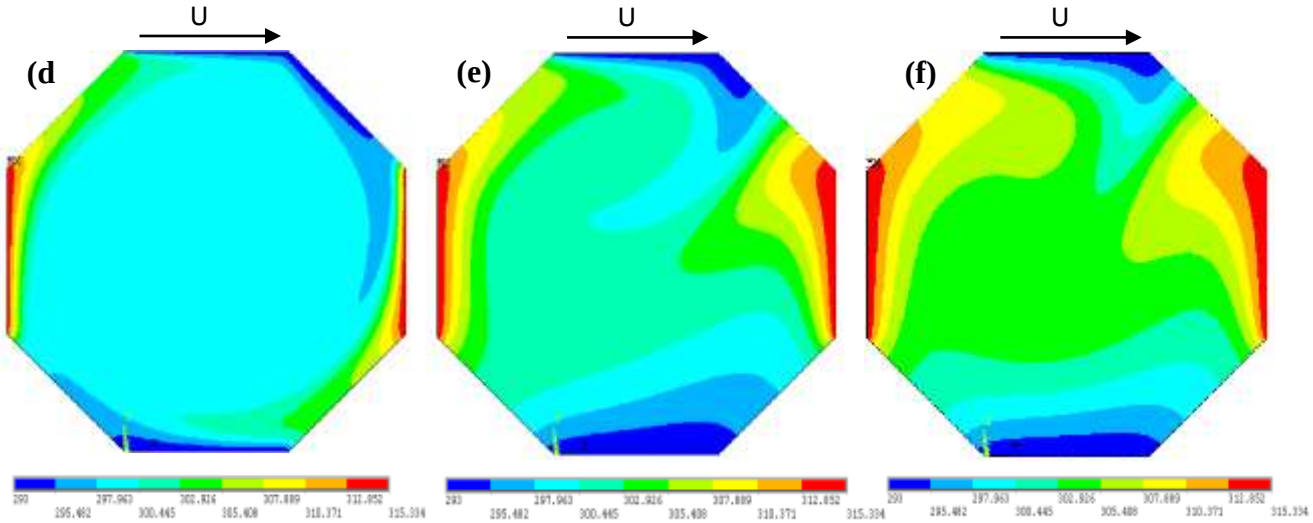

Isothermal body contour (Kelvin)

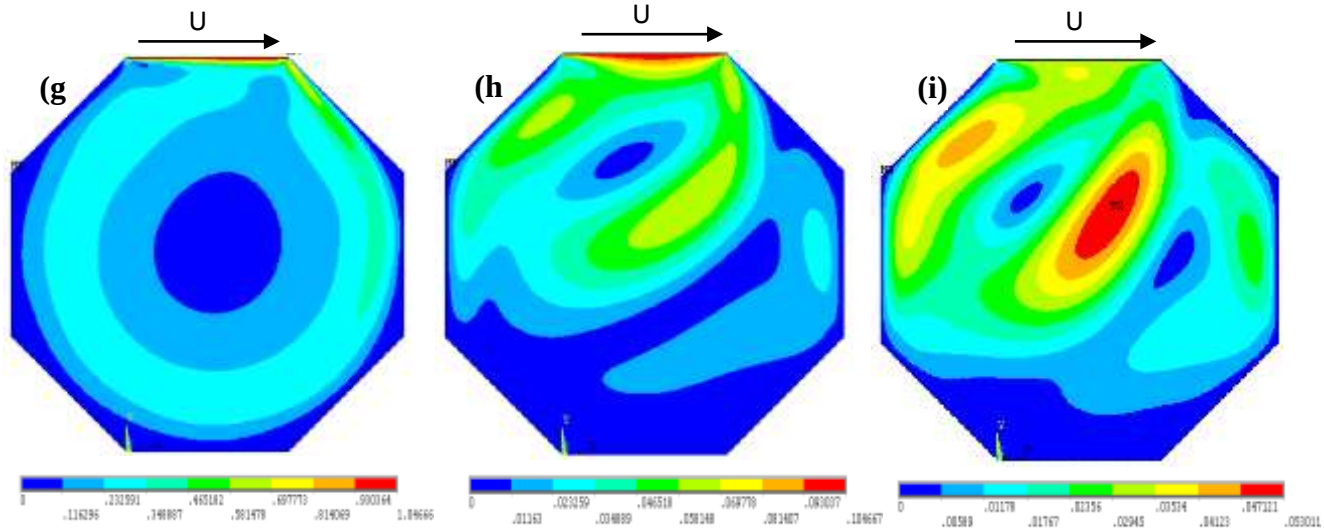

velocity distribution body contour (m/s)

Figure (4): Showing the streamlines, isotherms and the velocity body contours for top horizontal rightward motion of the lid driven motion with Ri = 0.01, 1, and 10.

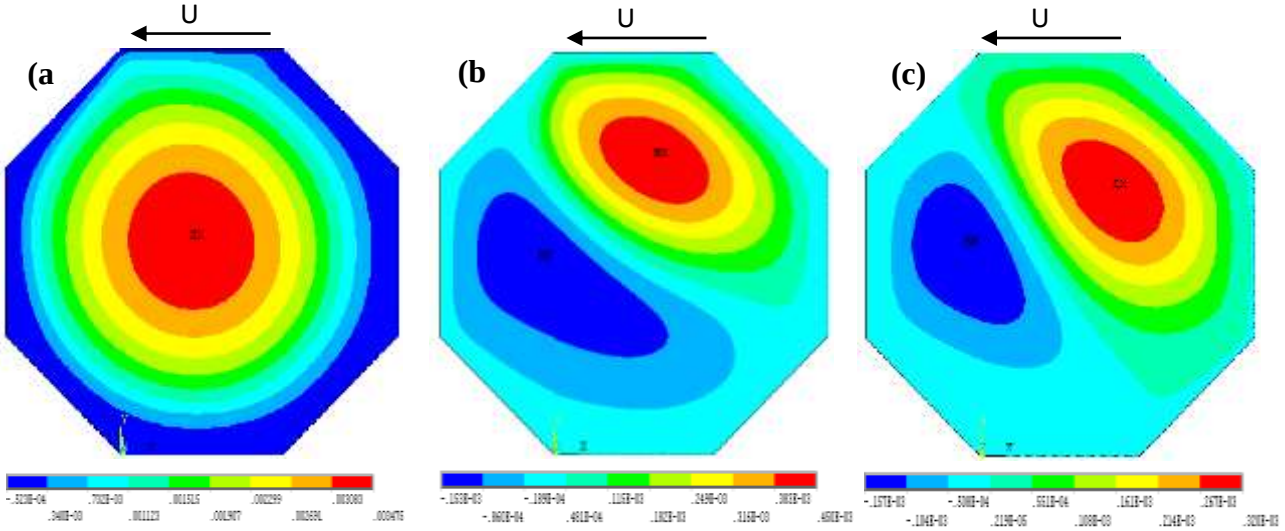

Stream function body contour (m^2/s)

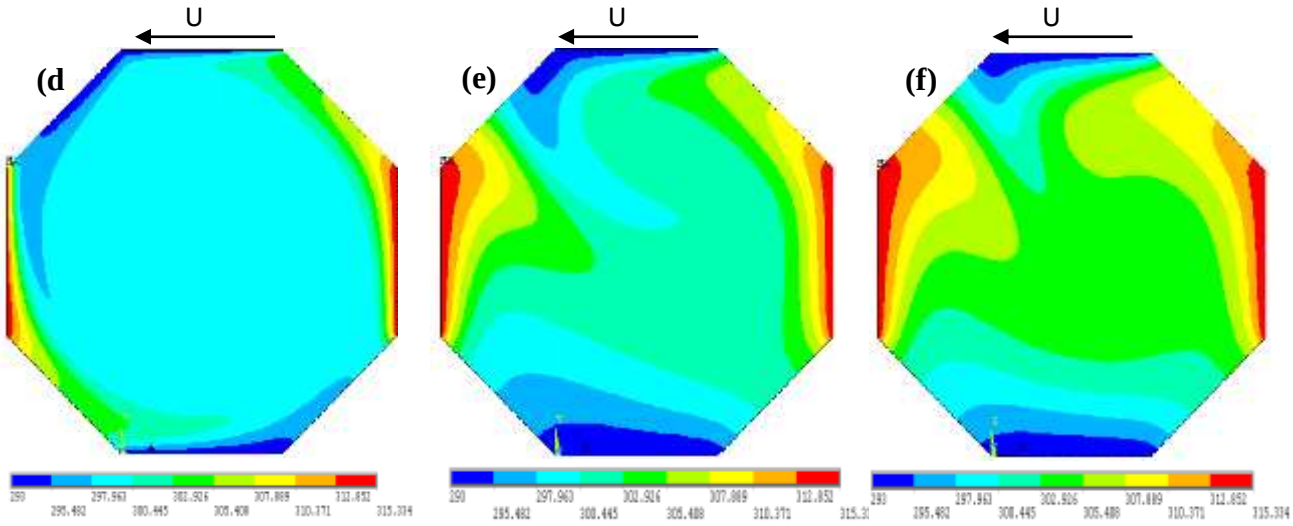

Isothermal Body Contour (Kelvin)

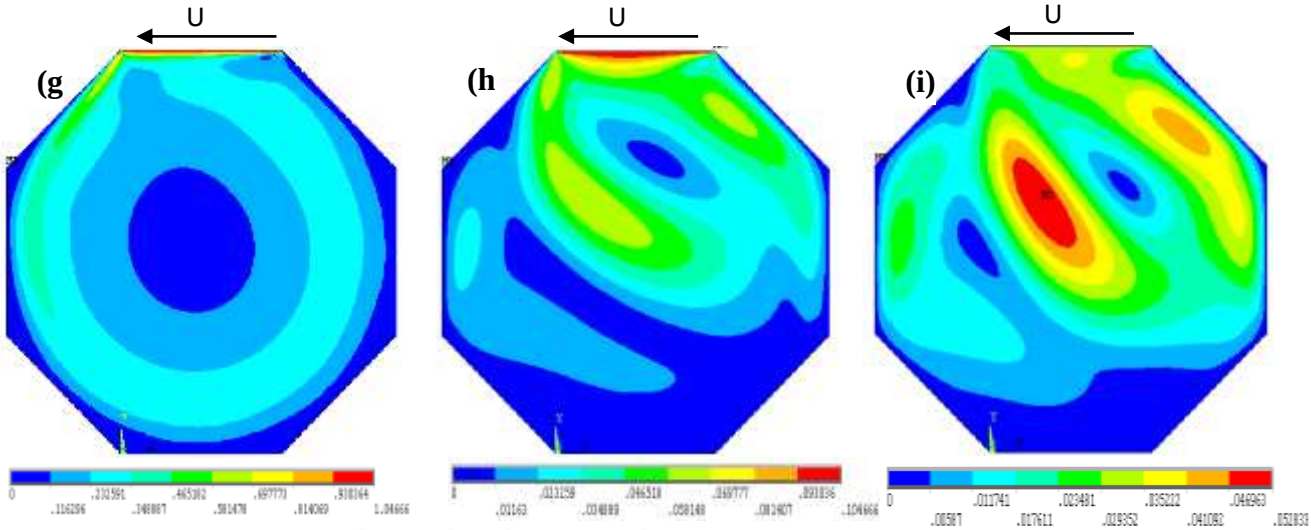

Velocity distribution Body Contour (m/s)

Figure (5): Showing the streamlines, isotherms and the velocity body contours for top horizontal leftward motion of the lid driven motion with Ri = 0.01, 1, and 10.

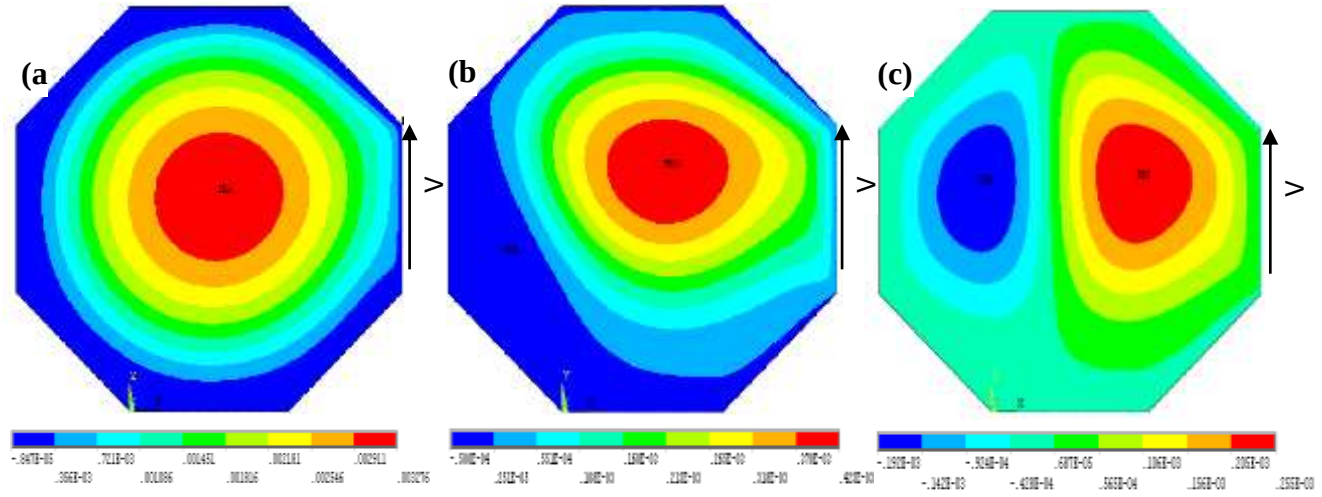

Stream function Body Contour

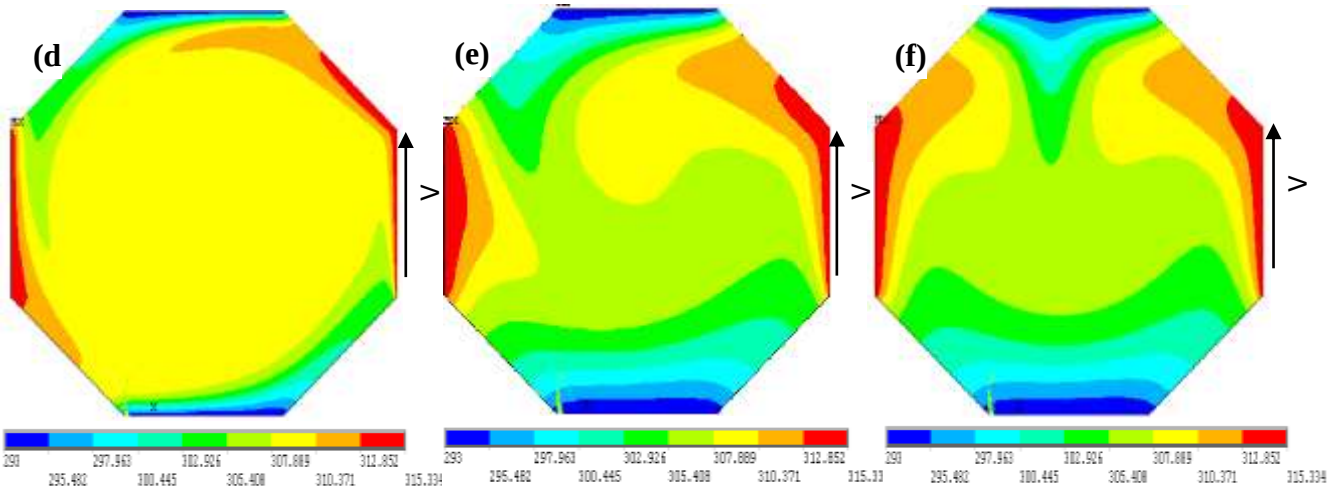

Isothermal Body Contour (Kelvin)

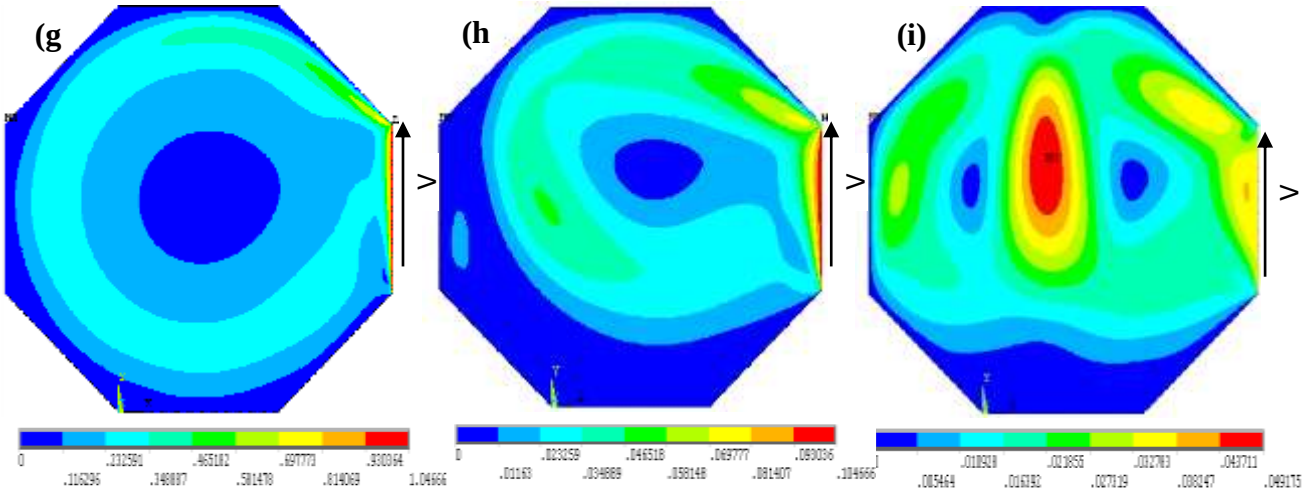

Velocity distribution body contour (m/s)

Figure (6): Showing the streamlines, isotherms and the velocity body contours for right vertical upward motion of the lid-driven motion with Ri = 0.01, 1, and 10.

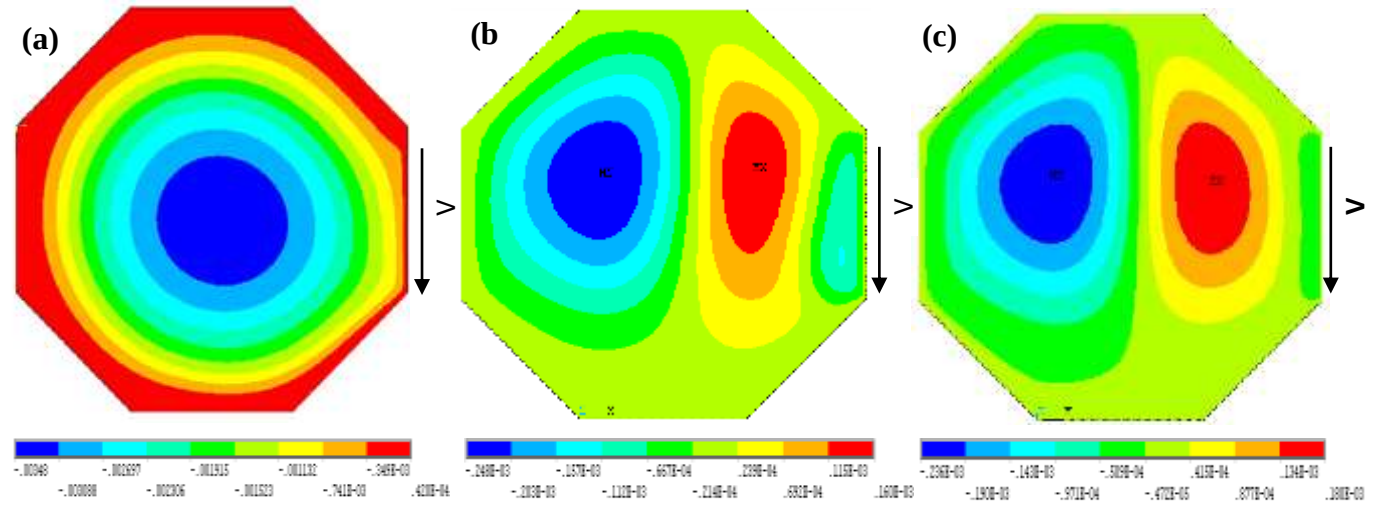

Stream function Body Contour

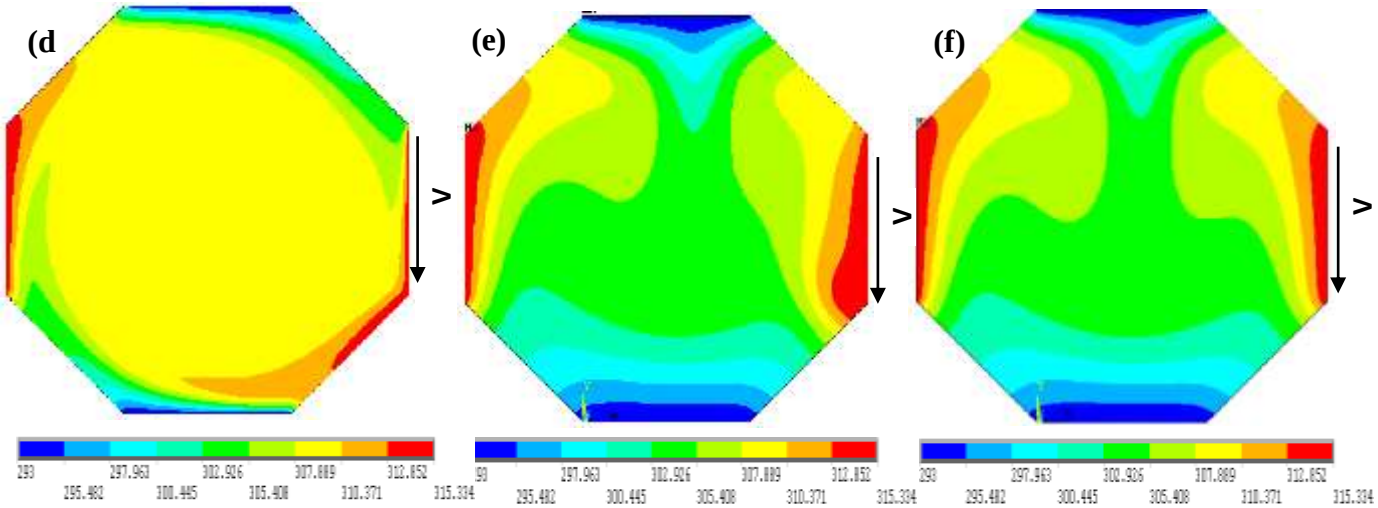

Isothermal Body Contour (Kelvin)

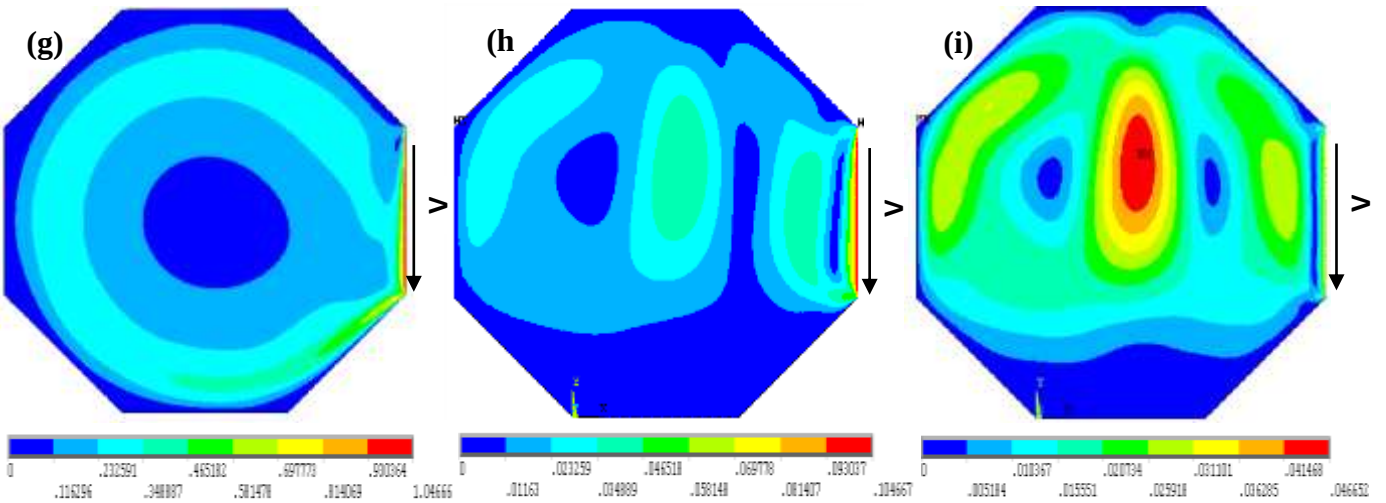

Velocity distribution body contour (m/s)

Figure (7): Showing the streamlines, isotherms and the velocity body contours for right vertical downward motion of the lid-driven motion with Ri = 0.01, 1, and 10.

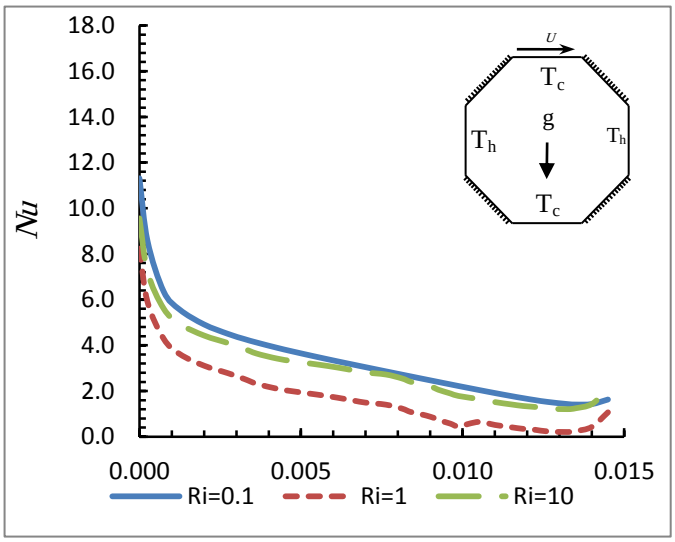

(a) Top horizontal rightwards motion of the lid driven

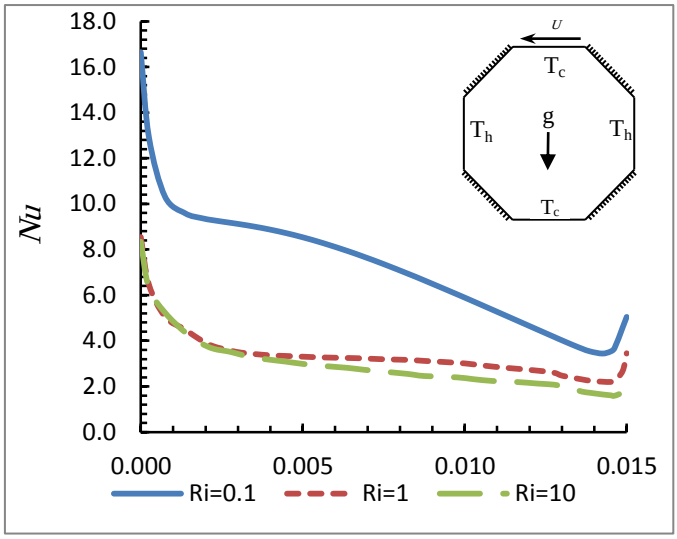

(b) Top horizontal leftwards motion of the lid driven

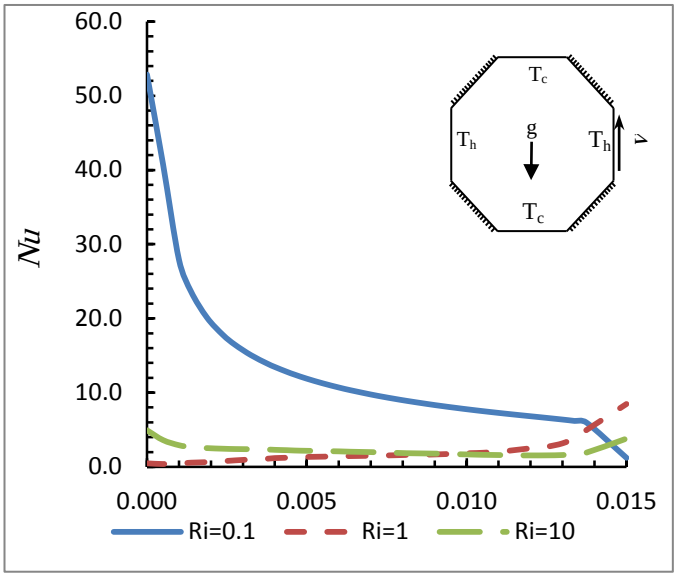

(c) Right vertical lid driven with moving upward

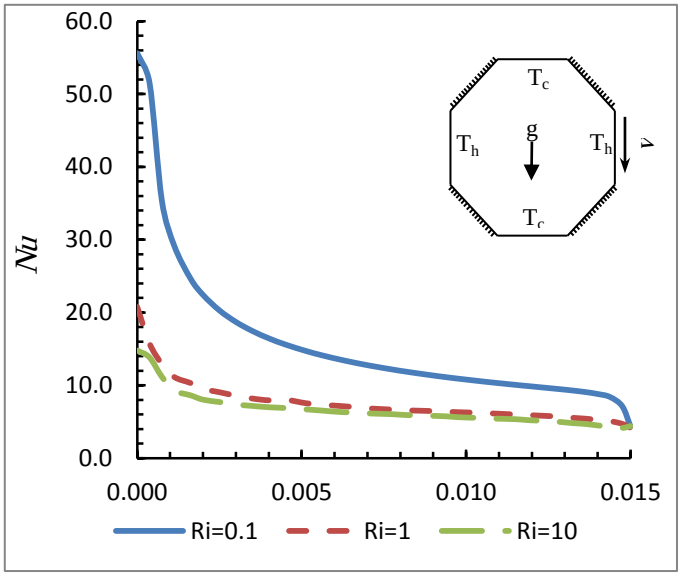

(d) Right vertical lid driven with moving downward

Figure (8): Variation of the local Nu along the hot right wall for cases 1, 2, 3, and 4 and Ri=0.01, 1, and 10.